SB^{3}C2016
Summer Biomechanics, Bioengineering and Biotransport Conference
June 29 –July 2, National Harbor, MD, USA

HEMODYNAMICS IN DEVELOPING STAGES OF CEREBRAL ANEURYSMS USING SPECTRAL-ELEMENT SIMULATIONS AND COMPARISON WITH PIV EXPERIMENTS

Tanvi K. Kaushik, Yulia T. Peet

School for Engineering of Matter, Transport and Energy
Arizona State University
Tempe, AZ, USA

Priya Nair, David H. Frakes

School of Biological and Health Systems Engineering
Arizona State University
Tempe, AZ, USA

INTRODUCTION

Aneurysms are pathological dilations of arteries; cerebral aneurysms are among the most dangerous ones and are commonly located in or near the circle of Willis [1][2]. The factors responsible for initiation, growth and eventual rupture of aneurysms have been identified as hemodynamics, wall biomechanics, mechano-biology and the peri-aneurysmal environment [1][2]. The rupture of this abnormality causes intra-cranial hemorrhagic strokes [1][2].

To compare the risks associated with surgery and the rupture of an untreated aneurysm, it is imperative to study the progression of its growth. In this paper we investigate the changes in hemodynamic quantities of three developing stages of aneurysm models through CFD simulations.

METHODS

Simulations were performed in an open source spectral element based CFD solver [3] Nek5000. Higher order spectral element methods with hexahedral mesh provide a better accuracy than the conventionally used finite volume codes that employ tetrahedral mesh [4]. The three developing stages of aneurysm models investigated in this paper are the advanced, mid and early stages. The advanced stage model was segmented and reconstructed from a patient-specific CT angiography dataset at the School of Biological and Health Systems Engineering (SBHSE) at ASU. This model was virtually modified to produce the early and mid stage models. Outlets and inlets for all the three models were extended to 10-15 times the diameter to allow for a better flow development and less interference with boundary conditions. The computational model of the advanced stage aneurysm with extended inlet and outlet is shown in Fig. 1. Hexahedral meshes were generated in the HyperMesh Software using mesh morphing tools. The numbers of elements in the early, mid and advanced stage models are 12760, 13946 and 15156 respectively, with 8 GLL points per element per direction in all the three directions. The numbers of nodes present in the three developing stages are 6533120, 7140352 and 7759872 respectively. Steady Poiseuille inflow conditions were applied at the inlet of all the three models. Simulations were executed for 0.7 seconds (600,000 time steps) with Reynolds number (based on mean inlet velocity and inlet diameter) equal to 653.21.

PIV experiments were performed at the SBHSE using a mixture of aqueous sodium iodide, glycerin and water. This blood analog was seeded with 8μm fluorescent microspheres.

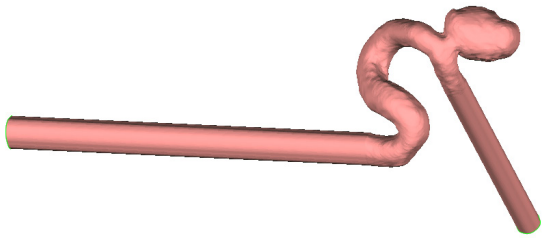

Figure 1: Advanced stage aneurysm model with extended inlet and outlet

RESULTS

Results from the PIV experiment and CFD simulation on the advanced stage aneurysm are compared in Table. 1. The center plane velocity profiles of the CFD and PIV models are shown in Fig. 2. The

velocity magnitude scale is non-dimensional, where 0.41 corresponds to 18 cm/s.

Table 1: Comparison of CFD and PIV root mean square velocity magnitude

Aneurysmal Quantity	CFD (cm/s)	PIV (cm/s)	Error (%)
Vrms	18.577	23.528	21.04

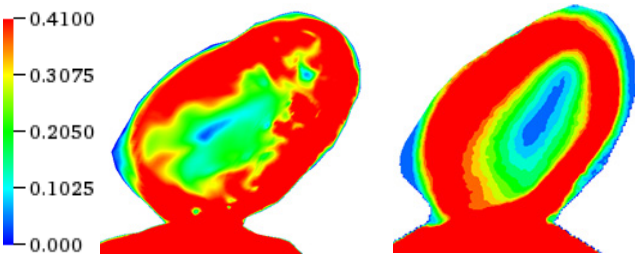

(a) CFD (b) PIV

Figure 2: Center plane velocity magnitude plot of the advanced stage aneurysm model

The following results have been obtained from CFD simulations. Center plane velocity vector plot of the early, mid and advanced stage aneurysm models are displayed in Fig. 3.

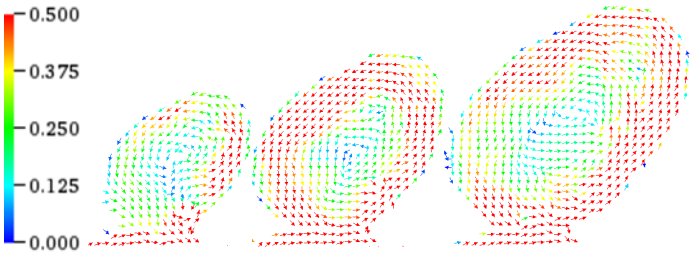

(a) Early (b) Mid (c) Advanced

Figure 3: Center plane velocity vector plot of the early, mid and advanced stage aneurysm models

Distribution of wall shear stress in the three stages is presented in Fig. 4

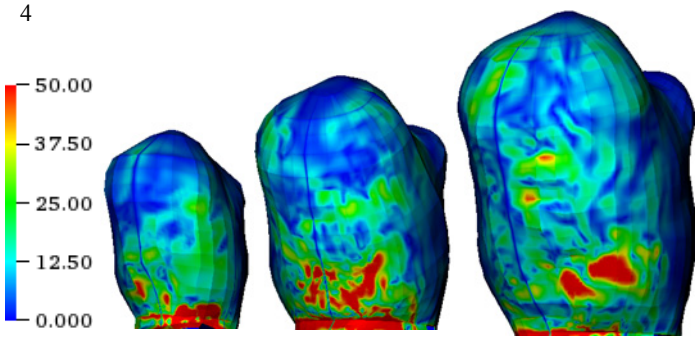

(a) Early (b) Mid (c) Advanced

Figure 4: Wall shear stress (Pa) in the developing stages

The weighted average values of hemodynamic quantities have been compared between the stages in Table. 2.

Table 2: Comparison of aneurysmal hemodynamic quantities in the three stages

Aneurysmal Quantities	Early Stage	Mid Stage	Advanced Stage
Vrms (cm/s)	14.192	20.524	18.577
WSS (Pa)	7.037	10.79	8.487
Pressure (Pa)	267.05	276.13	185.23

DISCUSSION

Local distribution of wall shear stress (wss) is governed by the swirling flow along the arterial walls. Circulation of fluid inside the curving geometry of the three models is noticeable in Fig. 3, although it is more distinct in the advanced and mid stages. Volume-averaged hemodynamic quantities in Table. 2 are seen to first increase between early-mid stages and then decrease between mid-advance stages. The initial increase could signify very early stages of aneurysm formation and flow development [1]. Reduction in values in the advanced stage is a consequence of wall enlargement, which is an adaptive response of the tissues to high blood flow [1]. Studies have shown that high wss regions initiate aneurysm formation as a response to the impact of inflow jets, and low wss regions are responsible for further remodeling and progression due to blood stagnation [1] and endothelial dysfunction [5]. Therefore it is important to identify both these regions, as seen in Fig. 4.

Results presented in this paper give us an insight into the flow dynamics in anatomically realistic aneurysm models. The two hurdles faced by such studies are, the necessity to perform these simulations at a time rate suitable for clinical decision making [6] and the requirement of physically-based parameters for predicting precise flow dynamics[6][7]. Also, further analysis of interaction among the aforementioned factors responsible for the growth and rupture is essential to gain a more comprehensive understanding of the disease.

REFERENCES

[1]Sforza, D. M., Putman, C. M., & Cebral, J. R., *Annual review of fluid mechanics*, *41*:91-107, 2009.

[2]Cebral, J. R., Putman, C. M., Alley, M. T., Hope, T., Bammer, R., & Calamante, F., *Journal of engineering mathematics*, *64*(4):367-378, 2009.

[3]Deville, M., Fischer, P., & Mund, E., "High-Order Methods for Incompressible Fluid Flow." *Cambridge University Press*, 2002.

[4]De Santis, G., et al., *Medical & biological engineering & computing*, 48(4):371-380, 2010.

[5]Boussel, L., et al., *Stroke,* 39(11): 2997-3002, 2008.

[6]Steinman, D. A., Milner, J. S., Norley, C. J., Lownie, S. P., & Holdsworth, D. W., *American Journal of Neuroradiology*, 24(4): 559-566, 2003.

[7]Castro, M. A., Putman, C. M., & Cebral, J. R., *Academic radiology*, 13(7):811-821, 2006.